



Simulation of groundwater flow paths under managed abstraction and recharge in an analogous sand-tank phreatic aquifer

Peipeng Wu^{1,2} · Longcang Shu^{1,2} · Changbing Yang³ · Yang Xu^{1,2} · Yongjie Zhang^{1,2}

Received: 11 July 2018 / Accepted: 13 August 2019 / Published online: 12 October 2019
© Springer-Verlag GmbH Germany, part of Springer Nature 2019

Abstract

Understanding the impacts of managed abstraction and recharge, i.e. artificial regulation of groundwater, on flow dynamics contributes to water resources planning and effective management of river basins. Based on the hydrogeological conditions of the aquifer in the Tailan River Basin, northwestern China, a two-dimensional sand-tank physical model and the corresponding numerical model were conceptualized and developed to investigate the influence of such regulation on the moisture content, groundwater flow patterns, groundwater age, residence time distributions, and groundwater flow paths in the groundwater reservoir. Four scenarios were examined at laboratory scale. The results showed that groundwater flow was influenced significantly by artificial regulation and that the depth of influence greatly increased depending on the regulation modes. Abstraction mainly alters the groundwater flow paths and moisture content at the ground surface in the core area of the depression cone and reduces the groundwater age in the entire aquifer. Groundwater flow lines are gradually parted by artificial recharge at different depths. Groundwaters of different ages have different behavior under the different artificial recharge depths and artificial recharge modes. Saddle points (kind of stagnation points) appeared at different locations, which were highly dependent on the modes of artificial regulation. Some of the lessons learned, and some management strategies, are proposed based on the results. Despite the dimensionality and scale of the model adopted, resulting in a relatively very large capillarity zone unrepresentative of field conditions, these findings nonetheless have important implications for understanding groundwater flow dynamics impacted by highly intensive human activities.

Keywords Groundwater flow paths · Abstraction · Artificial recharge · Infiltration basin · Laboratory experiments/measurements

Introduction

Groundwater is the primary source of potable water in many regions worldwide (Sawyer et al. 2016; Fan et al. 2013). During the few past years, over abstraction or persistent groundwater depletion occurs in many countries (Alley et al. 2002; Rodell et al. 2009; Wada et al. 2010, 2012; Gleeson et al. 2012). With difficulties in obtaining a sustainable long-term supply of

freshwater, caused by economic development, population growth, urbanization and irrigation-area increase (particularly in the arid and semi-arid areas), treated or treatable water is being injected and stored to preserve current water resources (such as flood water) for future use and sustainable development. This constitutes aquifer management (Frederick et al. 2014; Barker et al. 2016) and it is increasingly being viewed as a promising way to provide large storage capacity to capture seasonally or intermittently available excess water to meet water demands in the dry seasons and dry years (Dillon 2005, Dillon et al. 2006; Maliva et al. 2006; Vacher et al. 2006; Ward et al. 2009. Barker et al. 2016). This study focuses on groundwater reservoirs that present different issues compared with other aquifer management programs—i.e. artificial aquifer creation, aquifer recharge, aquifer reclamation, aquifer storage and recovery, aquifer storage transfer and recovery (American Water Works Association 2014, AWWA Manual M21 on Groundwater), and artificial recharge-pumping systems (Jonoski et al. 1997)—because the reservoir volumes studied

✉ Longcang Shu
lcshu@hhu.edu.cn

¹ College of Hydrology and Water Resource, Hohai University, Nanjing 210098, China

² State Key Laboratory of Hydrology-Water Resources and Hydraulic Engineering, Hohai University, Nanjing 210098, China

³ Environmental Data Techniques, Inc, 4515 Gardendale, BLDG 902, San Antonio, TX 78240, USA

here are larger. Groundwater, surface water, and ecological environments in a defined region are considered as an integrated system that takes account of managed abstraction and artificial recharge, collectively called ‘artificial regulation’ activity. A groundwater reservoir that is highly dependent on artificial regulation is regarded in terms of planning and management of the water resource, rather than merely a store of water.

The study of the hydrological response to human activities is an important topic in hydrology, to which many studies have contributed (Oki and Kanae 2006; Zhang et al. 2007; Barnett et al. 2008; Wang et al. 2009; Hotta et al. 2010; Jia et al. 2012; Bao et al. 2012; Yang et al. 2013; Deng and Chen 2017; Jakobczyk-Karpierz et al. 2017). The increasing demand for groundwater resources by human society in arid areas has altered natural groundwater hydrologic cycles (Erickson and Stefan 2009; Mi et al. 2016; Deng and Chen 2017; Gao et al. 2017). Many investigations, including field studies and numerical simulations, have shown that human activities such as groundwater pumping and urbanization have increasingly influenced groundwater levels (Ghaleni and Ebrahimi 2015; Mi et al. 2016), total groundwater storage (Wada et al. 2010; Mi et al. 2016) and groundwater quality (Keeler et al. 2016). While these studies have generated important insights into the effect of human activities on groundwater hydrological processes, few have evaluated changes in groundwater flow paths and the corresponding responses of hydrogeological processes. Characterizing groundwater flow paths is essential for understanding groundwater migration, which is very important for protecting regional water supply security, and for controlling dynamic behavior and hydrological cycles, as well as facilitating environmental conservation and water resources management (Nakaya et al. 2007; Polizzotto et al. 2008; Qin et al. 2012). Artificial regulation involves intensive activities to regulate water resources and represents a major factor in controlling the groundwater flow system on a regional scale. It is therefore necessary to analyze regional groundwater flow paths while considering extensive human activities, such as groundwater pumping and artificial recharge.

The aim of this study is to develop a sand tank model and conduct a numerical simulation model to investigate ambient groundwater flow paths in a groundwater reservoir area affected by artificial regulation activity. The sand tank model was established based on the hydrogeological conditions of the Tailan River watershed in northwestern China. Infiltration basins and injection wells at multiple layers were distributed near the upstream boundary, and pumping wells at different depths were located near the downstream boundary. Infiltration recharge was set using the site information. Laboratory experiments were conducted to investigate the flow paths and soil moisture content according to variations in hydraulic heads for different artificial regulation scenarios. Numerical simulations were conducted to simulate the

laboratory experiments and to quantitatively assess the effects of artificial regulation on ambient groundwater flow paths, the distribution of groundwater ages, the distribution of residence times and groundwater velocities under various artificial regulation modes.

Methodology

Site description

The field site is located at the Tailan River watershed (42°41′41″~42°15′13″N; 80°21′44″~81°10′14″E), in the southern piedmont of the western part of the Tianshan Mountains, in the north marginal zone of the Tarim Basin in Xinjiang autonomous region (Fig. 1). The climate of the Tailan Basin is classified as a continental arid climate, with an annual precipitation of 62 mm and evaporation of 1,840 mm. The Tailan River is primarily sourced by snowmelt water at the upper reaches of the Tarim River. According to the landform units along the river, the Tailan River watershed is divided into the intermountain depression zone, the alluvial fan, the alluvial plain, and the belt of transition between the oasis and desert. The slope plain areas at the piedmont (Figs. 1 and 2) have strong infiltration capacity, a deep water table, and higher recharge rate; the areas are rich in land resources, providing appropriate geologic and hydrogeologic conditions for the creation of a natural groundwater reservoir with resource potential. At the apex zone of the alluvial fan, the lithology of the geological formation is Quaternary gravels and coarse sand, and groundwater can be easily recharged through the unsaturated zone. Thick unsaturated zones can provide sufficient capacity to store surface water in the area. There is generally no connection between the stream and aquifer system, and between the infiltration basin and aquifer system (Deng 2012). The river and infiltration basin recharge groundwater via slow and diffuse seepage, depending on various physical factors that are directly related to topography, ecology, geology, and climate.

To some degree, alluvial fan areas are very suitable for the creation of natural groundwater reservoirs. Alluvial fans generally have a morphology that consists of three main parts from apex to apron: inner fan (short extension and coarse granulometry of deposits), mid fan (smaller grain size of particles and bed deposits), and outer fan (largest area made up by fine-grained bed deposits; Blair and McPherson 2009). These features (based on particle size, gradually changing from coarse to fine from apex to apron) could act as natural water-storage structures. The apex, which has highly permeable media, strong infiltration capacity and a deep water table, usually is the best area for artificial recharge projects. The apron, with low-permeability media, could act as an underground barrier to prevent the downflow of the artificially recharged water.

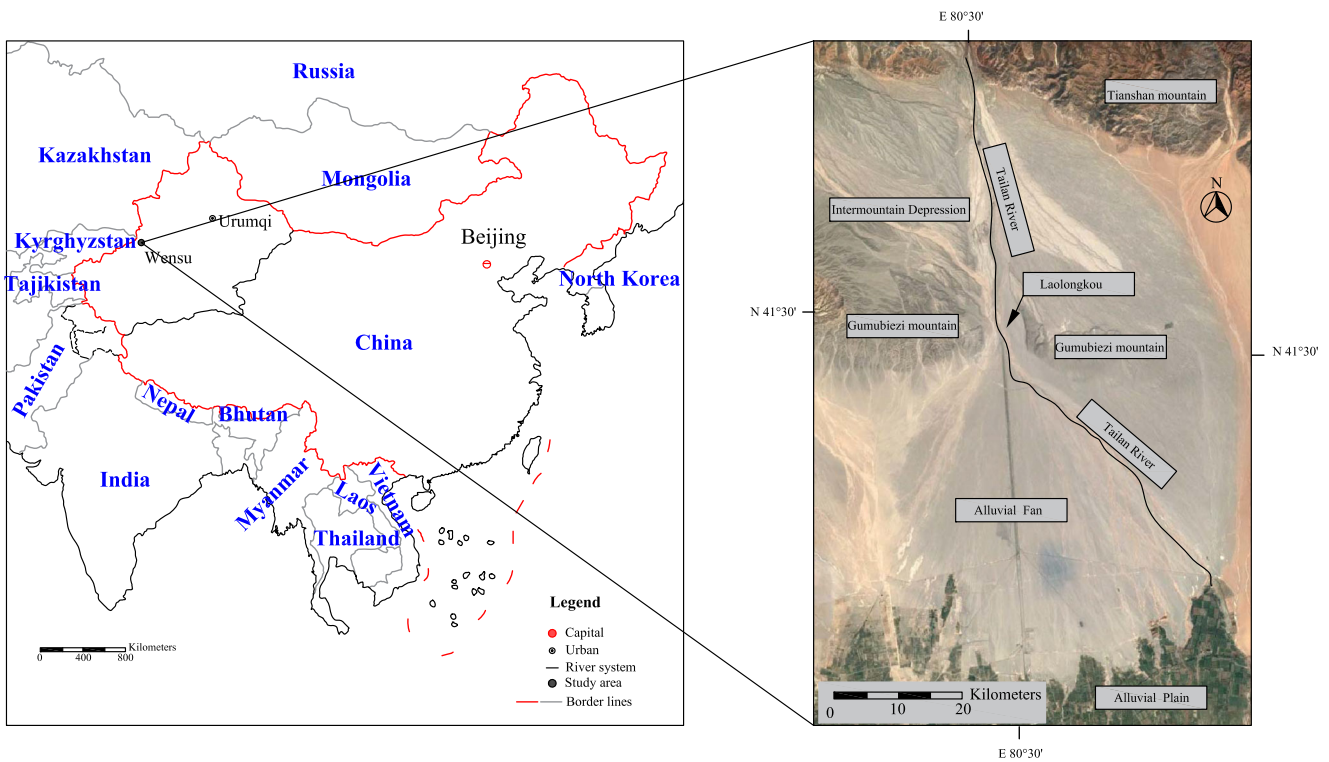


Fig. 1 The study area in the Tailan River Basin, Xinjiang, China

Laboratory experiments

A conceptual model of a groundwater reservoir was created, based on the hydrogeological conditions at the site (Fig. 3a). Laboratory experiments and the realization of the conceptual model were carried out with an acrylic glass tank measuring 2.05 m (length) × 0.5 m (height) × 0.16 m (width) to simulate a homogeneous phreatic aquifer (Fig. 3b). The sand tank was divided into three parts: the left-hand side was a reservoir representing the upstream constant head boundary, the middle part was filled with fine sands to simulate the loose sediments, and the right-hand side was another reservoir representing the downstream constant head boundary (Atlabachew et al.

2018). To mimic the actual hydrogeological condition in the apron area of the alluvial fan, where the first layer of the aquifer is a low-permeability medium and the deep layer is high permeability medium (Fig. 2), the right-hand boundary above the water level is set to be a no-flux boundary. Six computer-controlled pumps, each with a maximum pumping rate of 2.88 m³/day, were installed in two pumping wells (PW1 and PW2) and four injection wells (IW 1–4), respectively (Fig. 3a). In the physical experiments, well screen holes were made on the back face of the sand tank, which connected to peristaltic pumps. The discharging and recharging rates were measured continuously every 10 min. This physical model represents a cross section of the alluvial fan in a

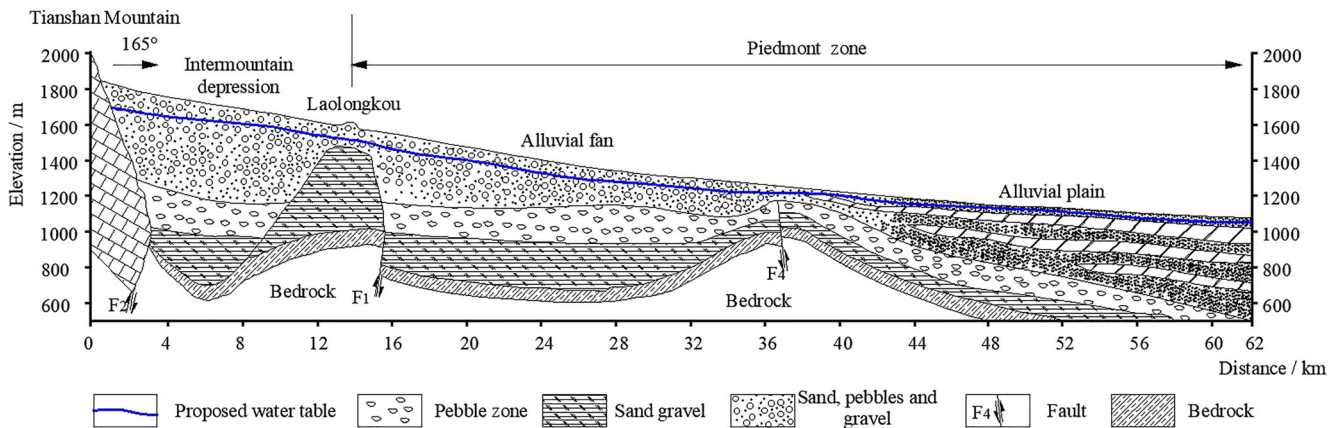


Fig. 2 Tailan River hydrogeological cross section showing the groundwater reservoir in the piedmont

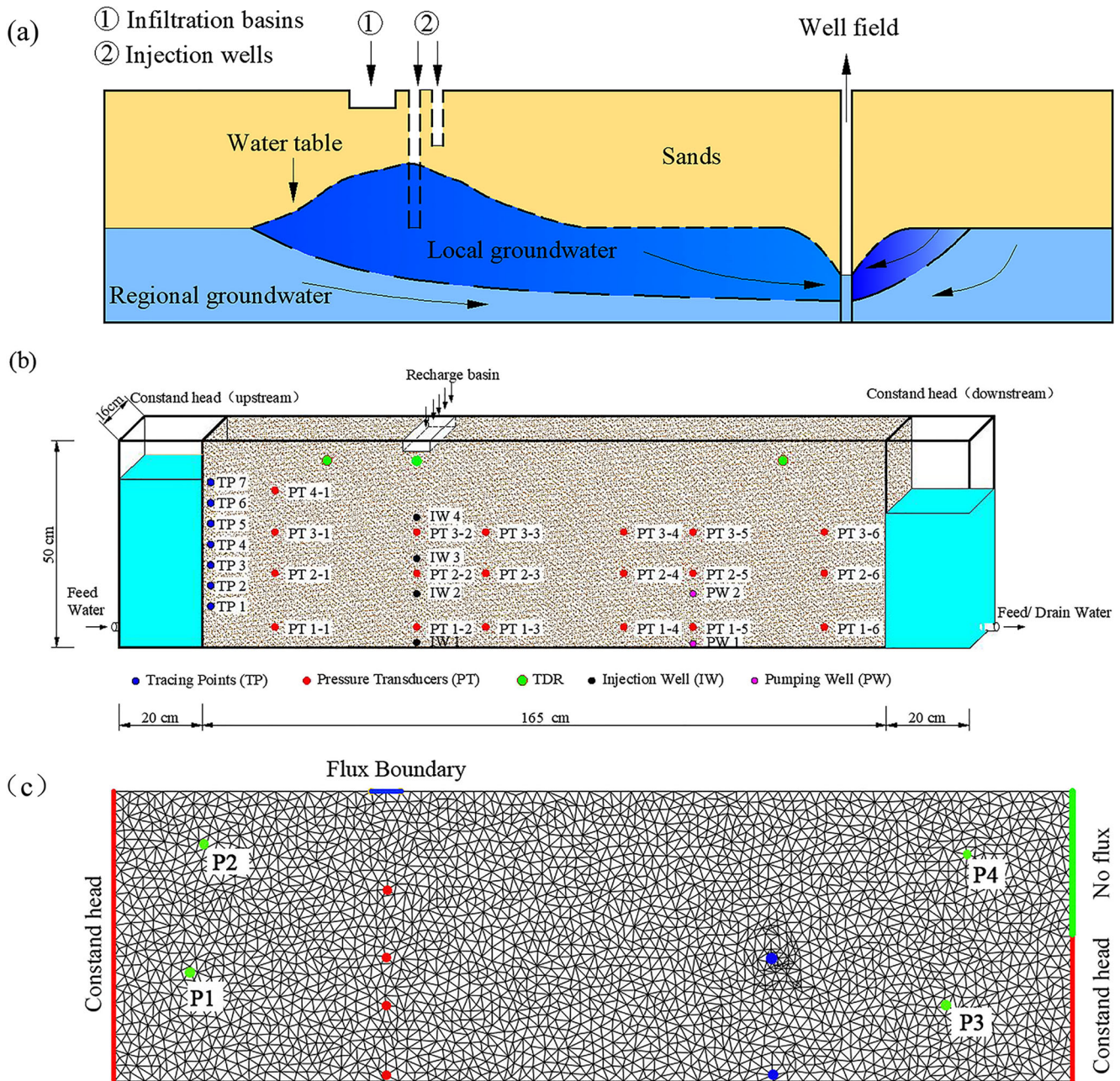


Fig. 3 **a** Conceptual model of groundwater reservoir; **b** schematic diagram of the sand tank and the experimental apparatus; and **c** side view of the laboratory-scale numerical model setup with prescribed boundary conditions. The boundaries on the right and left sides were set as a constant head boundary condition. The blue line (c) on the top boundary was set as a flux boundary condition. The four red points are

injection wells and the three blue points are pumping wells. The 19 red points (b) are the pressure transducers for the hydraulic head data acquisition. The four black points and two pink points (b) are the injection wells and pumping wells, respectively. The four green points are the calculation points of groundwater age

piedmont area in arid regions. Six vertical arrays of high-sensitivity deflated pressure transducers (PTs; HM20–1-A1-F2-W2, by German HELM; Fig. 3b) were buried directly into the tank to measure hydraulic pressure. These PTs were cabled to a time synchronized data-logger. Pressure measurements were collected every second.

The grain size distribution of the sand is shown in Fig. 4. The sand used in the experiments was relatively uniform with

$d_{50} = 534.6 \mu\text{m}$ and $d_{90}/d_{10} = 3.72$ ($d_{10} = 306.2 \mu\text{m}$; $d_{50} = 534.6 \mu\text{m}$; $d_{90} = 1138 \mu\text{m}$), which was optically determined using a LS Particle Size Analyzer by Beckman Coulter, USA, with a measurement range between 0.040 and 2,000 μm . The saturated hydraulic conductivity of the sand was 40.61 m/day as measured using the constant-head method and the bulk porosity was found to be 0.3 using the oven-drying method (Chinese National Standard, 1999). The

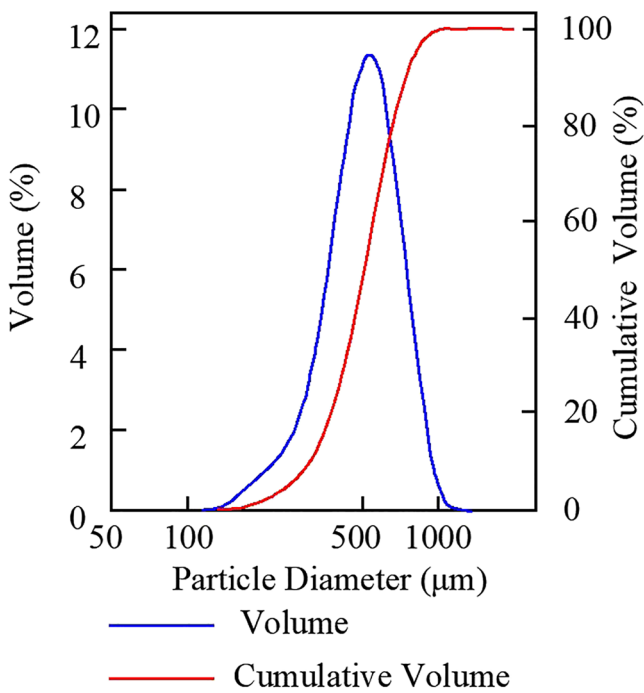


Fig. 4 The grain size (diameter, µm) distribution of the sands

permeability of the sands is substantially higher than that of typical fine sands in a natural state (Wilson et al. 2008), which is approximately 10 m/day.

To visualize ambient groundwater flow paths, seven tracing injection points were installed on the left of the middle part of the tank, and the tracer dye eosine (red) was added to the tracing injection points at a concentration of 0.3 g/L. The effects of the tracers on the density and viscosity of the fluid were assumed to be neglected (Stoeckl and Houben 2012). To analyze the development of the groundwater flow system, the experiment was recorded with a video camera at an interval of one frame every 10 min (Pixel 2400 W).

Scenarios of artificial regulation

Four different artificial regulation scenarios were considered, to mimic actual hydrological scenarios in the field (Table 1, scenarios A–D). Scenario A represents a natural condition with no artificial recharge and no groundwater abstraction. Three experiments were conducted for scenario A to examine the flow paths. The water levels were controlled at 43 and 25 cm above the inner base of the tank at the entrance (left) and exit (right) water chambers, respectively. The hydraulic gradient in the tank is justified according to the natural gradient in the Tailan River area, which is roughly consistent with the ground surface slope (0.06–0.1). Each of the three experiments started with a steady-state condition that was reached after approximately 180 min.

Scenario B represents a pumping condition with a constant pumping rate (pumping well) applied at a different depth of the aquifer. Two different pumping depths and three different

pumping rates (1.0, 1.5 and 2.0 m³/day) were conducted for scenario B to examine the pumping effect on groundwater flow paths. Because the groundwater reservoir is not in the Tailan River Basin, the infiltration rates were justified according to the water-table variations in the infiltration areas, which should not be higher than the upstream constant head. Pumping was initiated at different depths with a constant rate over a period of 180 min. The water levels in the upstream and downstream reservoirs in scenario B were fixed at the same as those in scenario A.

Scenario C represents a recharge condition with constant artificial recharge rates (infiltration basin) applied on the top of the aquifer. Three different experiments were conducted in scenario C using three different recharge fluxes (5, 10 and 15 m³/day) to examine the effect of infiltration basins on flow paths. The recharge area was located between distances of 39.6 and 49.5 cm away from the left Plexiglas screen separator. The recharge area was 0.016 m² with a 10 cm width and 16 cm length. Once the experiment began, a constant recharge was applied on top of the aquifer over a period of 180 min. The water levels in the upstream and downstream reservoirs in scenario A were applied to the reservoirs in scenario C.

Scenario D represents a hydrological condition with a constant injection rate (injection well) applied at different depths of the aquifer. Four different injection depths and three different injection rates (1.0, 1.5 and 2.0 m³/day) were conducted in scenario D to examine the effect of injection wells on flow paths. The water levels in the upstream and downstream reservoirs in scenario A were applied to this scenario. Furthermore, in order to avoid air trapping, wetting of the medium was always from the bottom, that is to say, experiments in all scenarios began with a slow rise in the water table.

Numerical model

FEFLOW (Diersch 2014), a variably saturated groundwater flow modeling program, was used for the numerical simulations. The basic equation (Diersch 2014) describing the groundwater flow simulated in the FEFLOW code is shown in the following.

$$sS_0 \frac{\partial h}{\partial t} + \varepsilon \frac{\partial s}{\partial t} + \nabla \times \mathbf{q} = Q + Q_{EOB} \tag{1}$$

$$\mathbf{q} = -k_r \mathbf{K} f_\mu \times (\nabla h + \chi \hat{\mathbf{e}}) \tag{2}$$

where s is the saturation of fluid in the void space ε [1], S_0 is the specific storage coefficient [L⁻¹], h is the hydraulic head [L], t is time [T], ε is the porosity (void space) [1], ∇ is the nabla (vector) operator [L⁻¹], \mathbf{q} is the Darcy velocity of fluid [L T⁻¹], Q is the bulk source/sink term of flow [L³ T⁻¹], Q_{EOB} is the correction sink/source term of the extended Oberbeck-Boussinesq approximation [T⁻¹], k_r is the relative permeability [1], \mathbf{K} is the tensor of hydraulic conductivity [LT⁻¹], f_μ is the viscosity relation function [1], χ is the buoyancy coefficient [1], $\hat{\mathbf{e}}$ is the gravitational unit vector [1].

Table 1 Definitions for different scenarios

Scenarios	Settings of different scenarios						
Scenario A	No artificial recharge and no groundwater abstraction						
Scenario B	Pumping	Pumping rates (m ³ /day)	PW1		PW2		
			1	B ₁	B ₂		
			1.5	B ₃	B ₄		
			2	B ₅	B ₆		
Scenario C	Infiltration basin	Recharge fluxes (m ³ /day)					
			5				
			10				
			15				
Scenario D	Injection	Injection rates (m ³ /day)	IW1	IW2	IW3	IW4	
			1	D ₁	D ₂	D ₃	D ₄
			1.5	D ₅	D ₆	D ₇	D ₈
			2	D ₉	D ₁₀	D ₁₁	D ₁₂

PW pumping well; *IW* injection well

B_n and D_n are the test numbers

The numerical model was built according to the experimental conditions shown in Fig. 3c. In particular, the following boundary conditions were applied. The base boundary was set as a no-flow boundary. The lateral boundaries on the right and left side (Fig. 3c) represent a constant head condition by the reservoirs and thus were set as a Dirichlet-type boundary. For the sediment surface, the nodes below the infiltration (red line in Fig. 3c) were set as the Neumann-type boundary. In the numerical model, the well screen was conceptualized to be a pumping point. The finite element mesh for the numerical solution is shown in Fig. 3c. The moisture-content/pressure relationships in the unsaturated zone were determined by the moisture contents combined with tensiometers and the van Genuchten (1980) equation. The van Genuchten parameters for all compartments were manually set to $\alpha = 4.05 \text{ m}^{-1}$ and $n = 1.987$.

The measured hydraulic head data together with the flow paths from scenario B were taken as an example to calibrate the model. In particular, the hydraulic conductivity and specific storage values were adjusted slightly using observed heads (Table 2). As an example, Fig. 5 shows the fitness between the measured and calculated heads using the trial-and-error method, suggesting that the numerical model is reliable for application. The flow paths simulated with the numerical model match well with the observed flow paths (Fig. 6).

Results

Moisture content

To examine the effects of artificial regulation on the moisture content in the groundwater reservoir area, the areas near the pumping wells, infiltration basin, or injection wells were assessed. The ground surface moisture content fluctuations were examined

at three locations: (30,50), (56,50) and (140,50). The moisture contents at the three areas of focus simulated in the numerical model for different scenarios are shown in Fig. 7. The moisture content decreased gradually along the vertical planes from upstream to downstream—for example in scenario A, the ground surface moisture content decreased from 0.278 to 0.228 along the vertical planes. Groundwater pumping led to a moisture content decrease from 0.2748 to almost 0.216 along the studied aquifer from upstream to downstream; notable is the area near the pumping wells in which the moisture content at 0.216 was smaller than that when pumping at the deep layer. This indicates that the effect of pumping in the central area of the cone of depression was intensified when groundwater was pumped at the shallow layer. However, the artificial recharge increases the soil moisture content, either in the infiltration basin or the injection well areas of the groundwater reservoir—for example, Fig. 7 shows that the ground-surface moisture content at the near upstream location increased from 0.278 to 0.285, whereas this content at the downstream location increased from 0.228 to 0.23. This led to an obvious deepening of the recharge layer for the moisture content driven by the infiltration basin compared with that by injection wells. The ground-surface moisture content at the downstream location increased from 0.230 to nearly 0.234 when transferred from the infiltration basin to injection at the deeper layer. Regarding the injection wells, the soil moisture content in the three areas of focus underwent no significant changes but slightly decreased with the deepening of the injection well screen.

Groundwater flow patterns and groundwater ages

Groundwater flow patterns for different scenarios are shown in Fig. 8. Simulation results show that for scenario A, without artificial regulation, the ambient groundwater flow directions were mostly horizontal. The velocity distribution in the sand

Table 2 Values of model parameters adopted in the laboratory and numerical simulations

Model type	Parameters			
	Hydraulic conductivity (m/day)	Anisotropic ratio	Specific yield	Porosity
Laboratory model	40.61	1	0.1	0.3
Numerical model	40	1	0.1	0.35

aquifer showed uniformity (Fig. 8a), primarily 4 m/day in the main part of the sand tank aquifer, which indicates that the hydraulic gradient dose not substantially change across areas of the sand aquifer.

Regarding the flow dynamic of scenarios under the stress of artificial regulation (Fig. 8, left panel), the important feature of the flow-net pattern is the existence of stagnant zones with extremely low or zero velocity. Stagnant zones are associated with saddle points, where groundwater velocity is zero. There are two saddle points in Fig. 8b, and where the shallow groundwater is abstracted, there is one saddle point, SP2 (located at the aquifer bottom). With a deepening in the pumping well screen, the saddle point in the saturated zone gradually disappeared. Under the stress of artificial recharge, saddle points can also appear at different locations in the upstream direction of the infiltration basin or injection well, indicated as SP3, SP4, SP5, SP6, SP7 and SP8, whereby SP4 is in an unsaturated zone, and the others are located in the saturated zone. Locations of saddle points were highly dependent on the forms of artificial regulation.

To better illustrate the stagnant zones, Fig. 9 zooms in on the flow patterns around SP2, SP6 and SP8. Taking the flow paths around SP 1 and SP8 as examples (Fig. 9a), it was found that streamlines flow in the opposite directions first and then converge to the same direction. However, regarding SP6, it was found that streamlines from upstream flow in the same direction first and then part toward opposite directions.

Velocity fields are also shown in the left panel of Fig. 8. The velocities of ambient groundwater flow driven by the abstraction could be increased significantly, especially in the saturated zone. Shown in the left-hand panels of Fig. 8a–c as the areas near the pumping wells, the velocities of ambient groundwater flow increased from 5 m/day under the natural state to approximately 10 m/day and were driven by pumping. It was concluded that the abstraction accelerates the ambient groundwater circulation rate in the groundwater reservoir area. Comparing the left-hand panel in Fig. 8a with that of Fig. 8d, the presence of the infiltration basin led to an obvious decrease in the groundwater flow velocities from 4 to 3 m/day in the upstream areas of the infiltration basin. Referring to the panels on the left in Fig. 8a,e,f,g,h, more obvious decrease of velocities appeared in the upstream areas of the infiltration basin as driven by the injection wells, where groundwater flow velocities decrease from 4 to ~0 m/day. Regarding the downstream areas of the artificial recharge projects, the groundwater flow velocities were found to increase from 4 to 5 m/day to ~5 to 7 m/day.

Groundwater age has also been further investigated, as shown in the right panel of Fig. 8. These figures show that groundwater abstraction and artificial recharge led to a decrease in the groundwater ages in the saturated zone. The groundwater ages in the unsaturated zone near the downstream boundary were increased by abstraction but decreased by artificial recharge. To obtain further insight into the

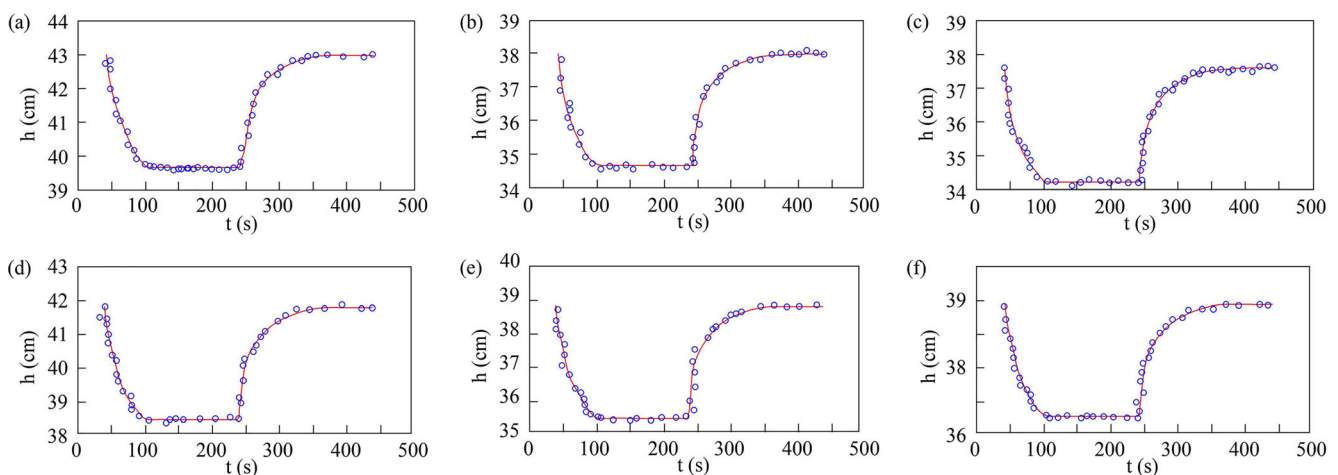


Fig. 5 Comparison of simulated and measured groundwater head variations for scenario B using parameter values shown in Table 2. The red lines are simulated results and the blue point are measured results. **a** Measured and simulated at TP 1–1, **b** measured and simulated at TP 1–3,

c measured and simulated at TP 1–6, **d** measured and simulated at TP 2–4, **e** measured and simulated at TP 3–3, **f** measured and simulated at TP 4–1

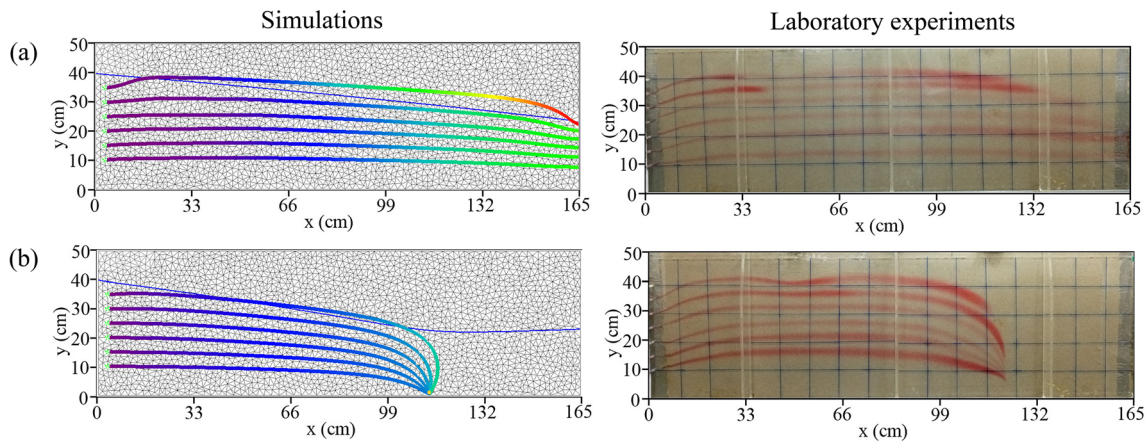


Fig. 6 Comparison of the **a** simulated flow path lines associated with travel times and **b** measured path lines under scenario D. The left panels are for numerical simulations and right-hand panels are for laboratory experiments. All the figures reflect stable conditions

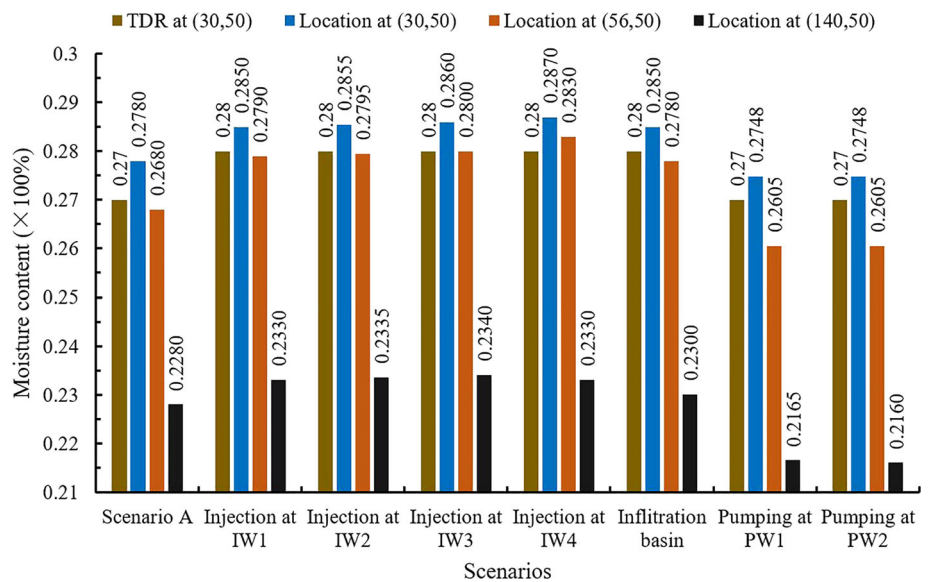
groundwater ages, four calculation points were set at different locations in different scenarios. The four calculation points were $P_1(12, 20)$, $P_2(15, 43)$, $P_3(143, 14)$ and $P_4(146, 38)$. Groundwater ages at the steady-state condition driven by artificial regulation activities are displayed Fig. 10. P_1 and P_3 were located at upstream and downstream positions of the saturated zone, respectively, whereas P_2 and P_4 were located at upstream and downstream positions of the unsaturated zone, respectively. Figure 10 shows that the injection wells increased the groundwater age in the upstream areas and decreased the groundwater age in the downstream areas. With the deepening of the injection well screen, the groundwater age in the saturated zone in the upstream area became longer but shortened in the unsaturated zone in the upstream area. In the downstream areas, with the deepening of the injection well screen, the groundwater age became longer both in the saturated and unsaturated zones. Influenced by the infiltration basin, the groundwater age in the whole aquifer became shorter

compared with that in the natural condition. Groundwater abstraction decreased the groundwater age in the upstream areas but increased that in the downstream areas. The groundwater age became shorter with the deepening of the pumping well screen.

Residence time distributions

Residence time distributions (RTDs) of the sand tank phreatic aquifer in different scenarios are considered here. The results show that not only the ambient groundwater driven by artificial regulation but also the artificial recharged water exhibit different RTD laws compared with the natural state. The frequency distribution (FD) of the ambient groundwater and artificial recharged water’s RTDs show clearly different progressions in different scenarios (Figs. 11, 12, and 13). Most FDs of the ambient groundwater’s RTDs are driven by artificial recharge toward an exponential law behavior with a changing depth of artificial

Fig. 7 Moisture content fringes simulated with the numerical model for different scenarios



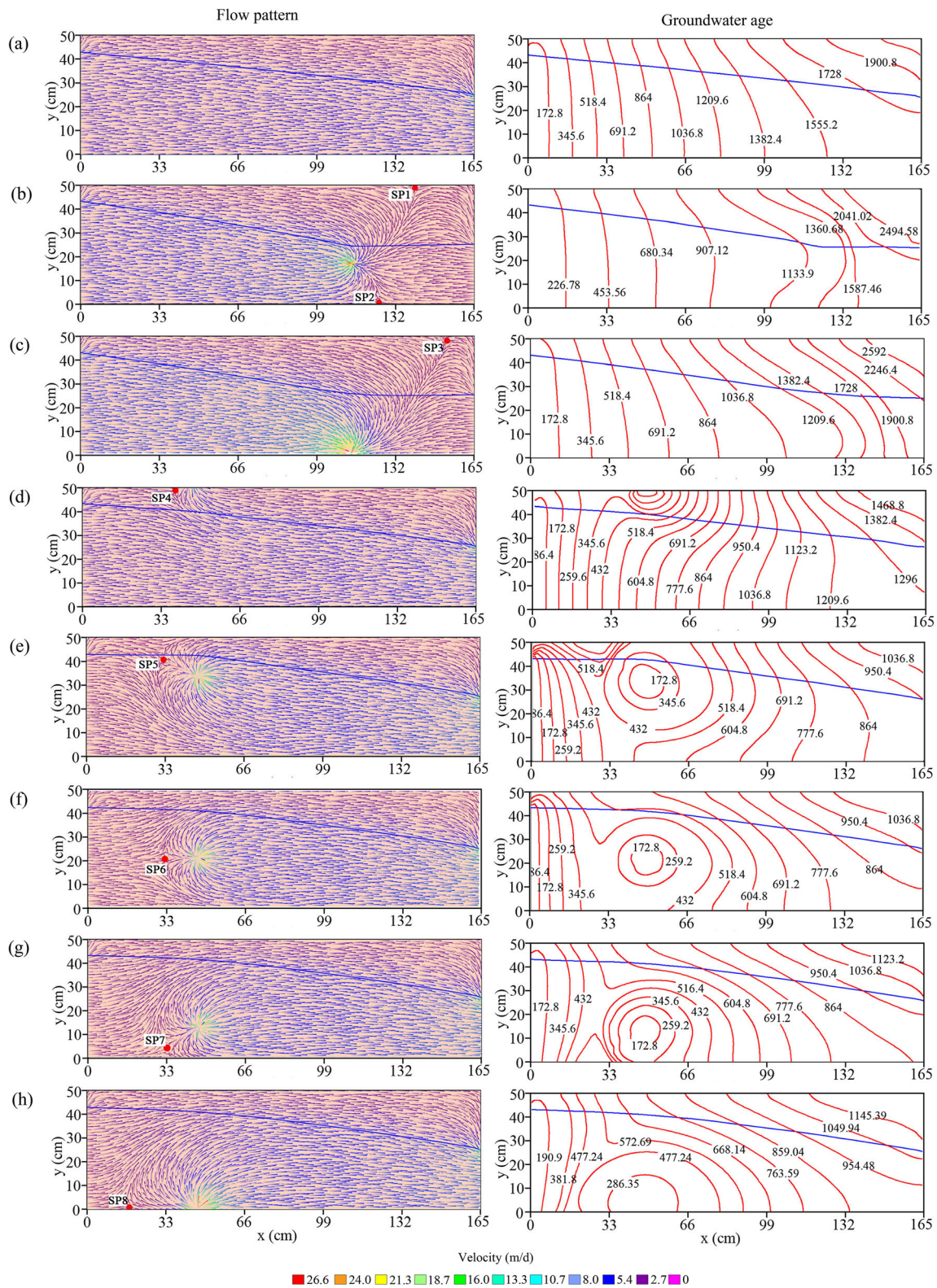


Fig. 8 Flow patterns (left panel) and groundwater age (right panel, the unit is second) from numerical simulation under **a** scenario A, **b** scenario B pumping at PW2, **c** scenario B pumping at PW1, **d** scenario C, **e**

scenario C inject at IW4, **f** scenario C inject at IW3, **g** scenario C inject at IW2, **h** scenario C inject at IW1. In the right panel, the blue lines are the water table, and the red lines are groundwater ages

recharge, except for these injected by IW1 and IW3, which tended toward logarithmic law. However, overall, the shapes of

the FD of the ambient groundwater’s RTDs driven by artificial recharge do not show substantial change according to the depth

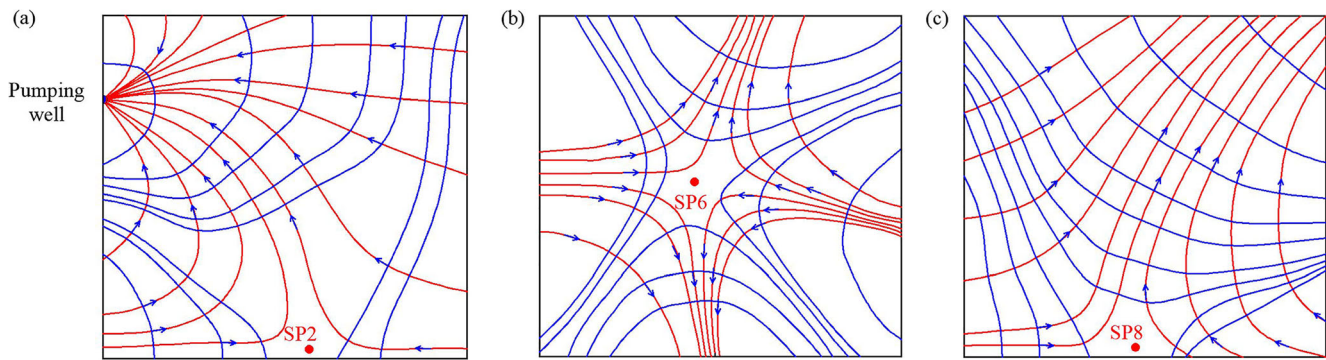


Fig. 9 Distribution of hydraulic head (blue lines) and streamlines (red lines) around saddle points SP2, SP6 and SP8

of artificial recharge (Fig. 11). Most of the FD of the artificial recharged water's RTDs shows a logarithmic law behavior with a changing artificial recharge depth, except for those artificially recharged by the IW4 and infiltration basin, which tended toward exponential law. The early time portion of the FD of the artificially recharged water's RTDs shows a very clear progression toward a step-like change. In other words, the frequencies of the artificially recharged water's residence times are nearly equivalent to each other in this portion, primarily from approximately 2,000–5,000 s (Fig. 12). In Fig. 13, the FDs of ambient groundwater's RTDs show very different behaviors under the abstraction at different depths. Deep pumping leads to the FD of ambient groundwater's RTDs toward a logarithmic law behavior, and shallow-depth pumping leads to a polynomial motion.

Ambient groundwater flow paths

Particle tracking was used to examine the effect of artificial regulation on ambient groundwater flow paths. Several particles were released at different points in the numerical model on the left side to trace the ambient groundwater flow (Fig. 14, left panel). Particles were released from the same locations at

the steady-state conditions in different scenarios. At the same time, flow nets (Fig. 14a–h, right-hand panels) based on the hydraulic heads by pressure transducers at steady-state conditions were also produced after the laboratory experiments. The penetration depth of the ambient groundwater flow from TP1 and TP6, at the section of $x = 99$ cm are also shown in Fig. 15. In contrast with the definition of penetration depth by Zijl (1999) based on the decay of flux intensity, the penetration depth of groundwater flow here is the depth of certain groundwater flow paths at certain sections.

The variations in groundwater flow paths for scenarios A–D are shown in Fig. 14. The results from both laboratory experiments and numerical simulations show that the artificial regulation greatly changed the ambient groundwater flow paths. The effect of abstraction on ambient groundwater flow paths mainly occurred in the cone of depression. The abstraction at a shallow layer shallowed the penetration depth of the groundwater from the deep layer and deepened the penetration depth of the groundwater from the shallow layer in the cone of depression (Fig. 14b). With the deepening of the pumping well screen, the penetration depth of the ambient groundwater from deep layers increased in the cone of depression (Fig. 14c).

Fig. 10 Groundwater ages at different locations in different scenarios. The numbers at the top of the bars are groundwater ages (seconds)

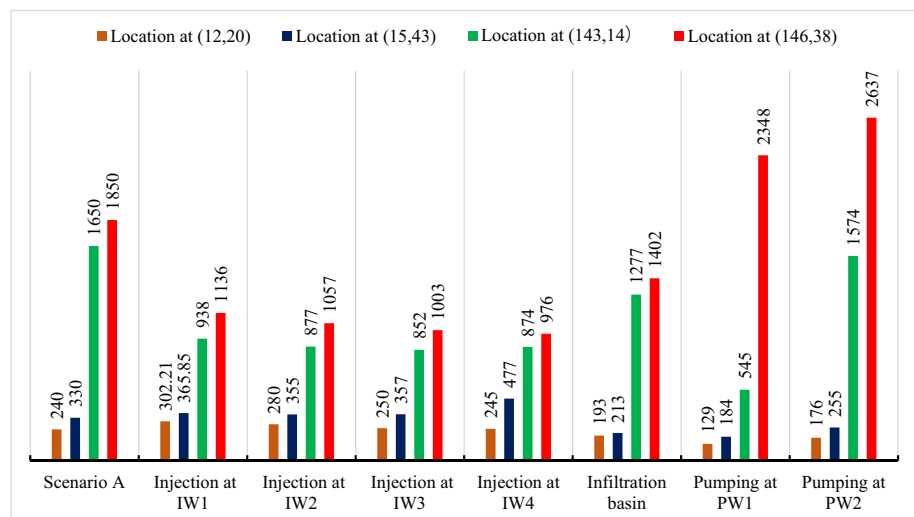
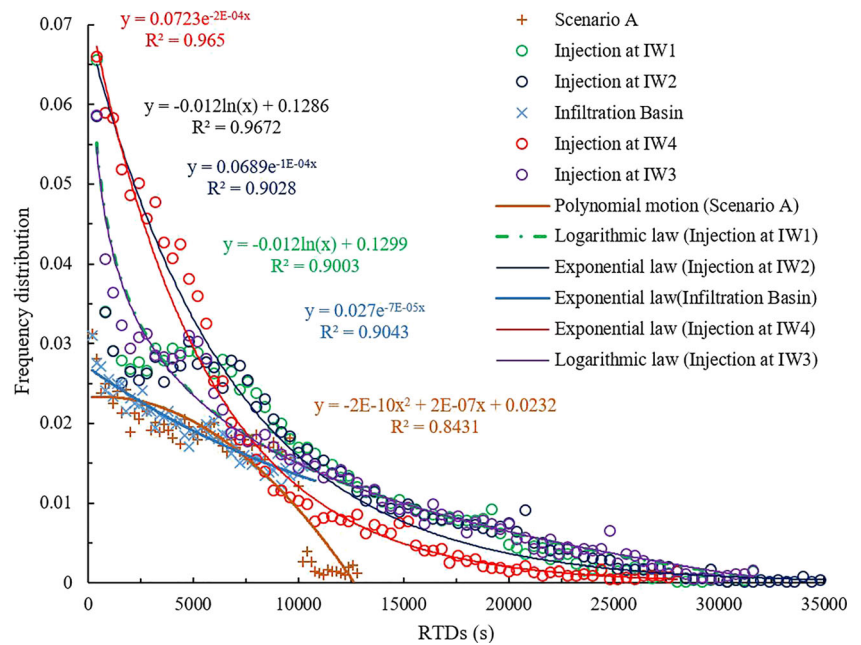


Fig. 11 Frequency distribution of residence time distributions (RTDs) for ambient groundwater and its fitted trend lines under the driver of artificial recharge



The effect of the law of artificial recharge on the ambient groundwater flow paths relies on the artificial recharging method (infiltration basin, injection well, recharging intensity, etc.). In scenario C, artificial recharge was set as a localized constant artificial recharge flux (infiltration basin), applied on the surface of the aquifer. Figure 14d shows the ambient groundwater flow paths at the steady-state condition when the recharge flux is 10 m³/day. The infiltration-basin effect induced increased penetration depth of the ambient groundwater flow increase. In scenario D, artificial recharge was set as a constant injection rate (injection well) applied at different depths of the aquifer. Four different injection depths and three different injection rates (1.0, 1.5, and 2.0 m³/day) were conducted in scenario D to examine the effect of the injection well (including the injecting depth and rate) on ambient groundwater flow. Figure 14e–h shows the

results of scenario D. When the injection well screen was located in the shallow layer, the penetration depth of the ambient groundwater flow increased. With a deepening injection well screen, the ambient groundwater flow was gradually fractionated by artificial recharge. When the injection well screen was in the bottom layer, the penetration depth of the ambient groundwater flow decreased.

Discussion

This study developed a physical sand-tank model and a corresponding numerical simulation model to investigate the ambient groundwater flow paths as expected to take place in a groundwater reservoir area affected by artificial regulation.

Fig. 12 Frequency distribution of RTDs for artificial recharged water and its fitted trend lines

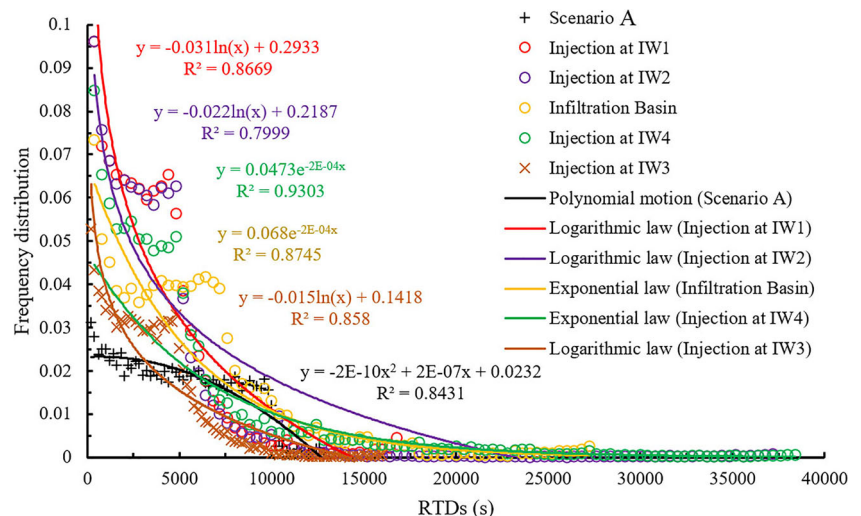
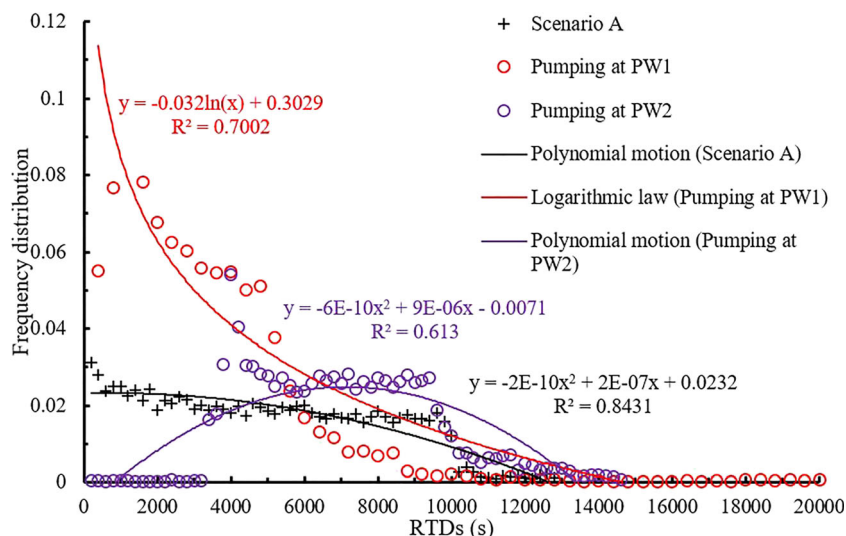


Fig. 13 Frequency distribution of RTDs for ambient groundwater under the driver of pumping and its fitted trend lines



The groundwater recharge and discharge elements and their circulation patterns were collected and calculated based on data from the Tailan River watershed, which is located in an arid area. The real utility of this sand tank and numerical model is to simulate the variation in the ambient groundwater flow system under different conditions with varying artificial regulation modes. In this study, artificial regulation modes were represented with the infiltration basin, injection wells and pumping wells (Andrew et al. 1999; Konrad et al. 2014; Emily et al. 2016; Ebrahim et al. 2016). Practically, surface water flowing through alluvial fans in arid and semiarid areas are often disconnected from groundwater; that is, an unsaturated zone between the surface water and ambient groundwater is gradually produced when the stream is disconnected from the aquifer (Wang et al. 2011, 2014; Newcomer et al. 2016). Thus, the infiltration basin was set as a prescribed flux (Neumann type) boundary (Carabin and Dassargues 1999). A total of 19 high-sensitivity deflated PTs were buried at different locations of the sand tank to measure the hydraulic gradient. The hydraulic gradient data were collected once per second. The pumping rate and injection rate could be stabilized by seven computer-controlled pumps. Tracer dye was added to the ambient groundwater during the laboratory experiments. Despite the difference of dimensionality and scale of the models as compared to the field case study, these settings effectively satisfy the study of ambient groundwater flow paths driven by artificial regulation. Admittedly, the limitation of using the small-scale model would lead to some unreasonable results—for example, the capillary zone thickness relative to the saturated zone thickness is extremely large in these experiments, which seems unreasonable when considering a field-scale case. The limitation, however, does not affect the main purpose of this study (i.e., understanding how pumping and recharge affect the ambient groundwater flow dynamics).

The method regarding the images was developed by Bear (1979) to solve the well flow problem influenced by the

boundary in the analytic method. When the wells with short pumping or injection times are far from the boundary and the boundary does not have an obvious influence on the well flow during the process, it can be treated as an infinite aquifer. However, the existence of the boundary must be considered when the well is near the boundary or in the case of long-term pumping or injection, where the boundary has a significant effect on the flow. In this condition, the single well could act as a line of wells when determining the flow field in the analytical method. In this study, the simulated groundwater flow by laboratory experiments is generally three-dimensional (3D), especially in areas near the infiltration basin, injection well, and pumping well screens. As Oostrom et al. (1992) reported, flow instability is inherently 3D and time-dependent, even in a relatively narrow sand flume as that used in this study. Before the fingers at the front side reached the bottom of the tank, those at the back had reached the pumping well (Fig. 6b). On the other hand, a tracer test could visualize groundwater flow in the sand tank under certain conditions, but the dispersion effect could also seriously influence the results. Therefore, in this paper, the flow fields were mainly produced using hydraulic head values collected by a pressure transducer; however, due to symmetry, the flow on the vertical plane along the model's center line is two-dimensional (2D). Since key flow characteristics are expected to be 2D in the vertical and horizontal directions, the discussion will be first focused on such 2D flows. Overall, the results from the laboratory experiment and numerical simulation agreed reasonably well with each other (Fig. 6).

Notably, due to the scale effect, some of the derived results are unusual—for example, the circumstances that allow the possibility of upward flow across the water table in this experiment seem impossible, which is also shown by the results of the tracer test in Fig. 6. The upward flow is mainly driven by the gradient and hydraulic conductivity of the unsaturated zone. The hydraulic conductivity of the unsaturated zone is

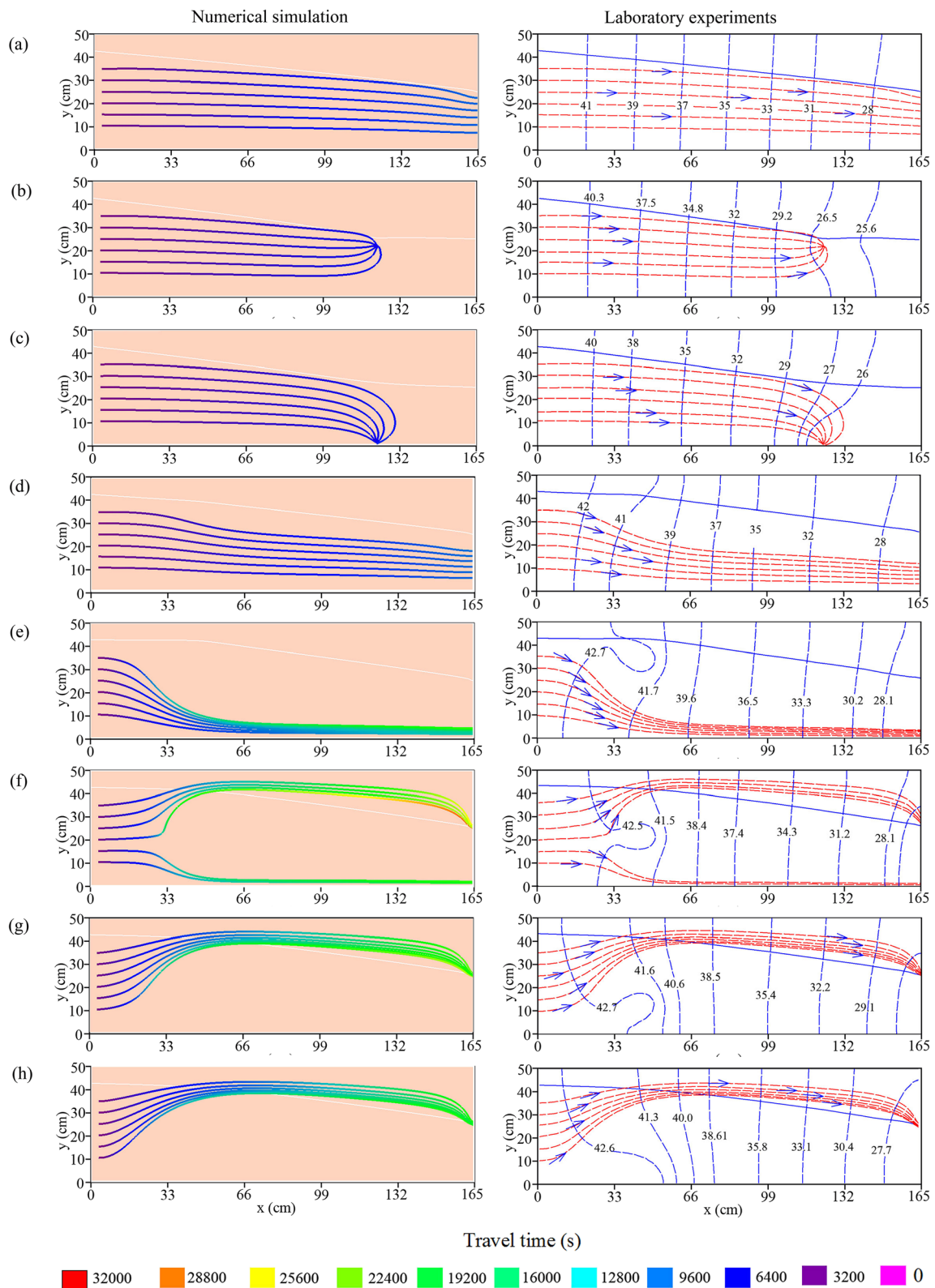
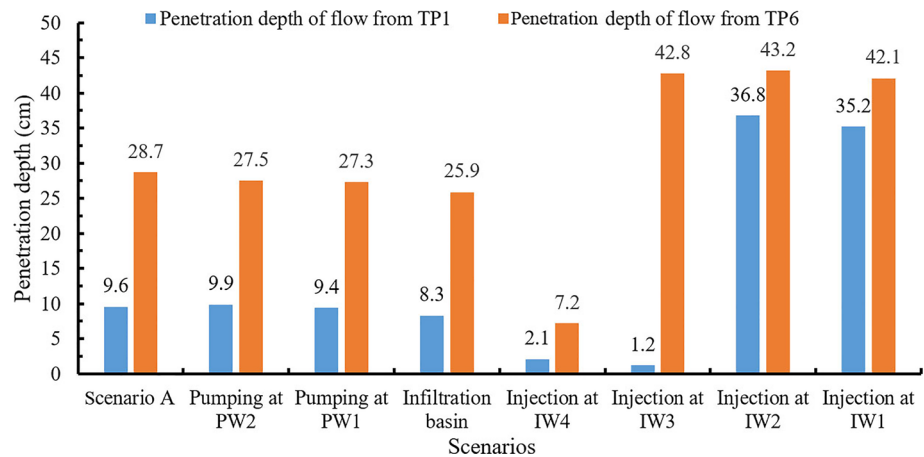


Fig. 14 Path lines associated with travel time from numerical simulation (left panel) and path lines from laboratory experiments (right panel) under **a** scenario A, **b** scenario B pumping at PW2, **c** scenario B pumping at PW1, **d** scenario C, **e** scenario D inject at IW4, **f** scenario D inject at IW3,

g scenario D inject at IW2, **h** scenario D inject at IW1. In the left panel, the white lines are the water table. In the right panel, the blue lines are hydraulic heads, the red lines are flow paths and the blue arrows are flow directions

Fig. 15 Penetration depth of ambient groundwater flow from TP1 and TP6, at the section of $x = 99$ cm



controlled by the water content. The greater the water content, the larger the hydraulic conductivity of the unsaturated zone. Numerical simulations and measurements shown in Fig. 7 indicate a high degree of saturation throughout the sand tank, suggesting that the hydraulic conductivity of the unsaturated zone is close to that of the saturated zone. Capillary fringe thicknesses are controlled by the particle size and void diameter. The finer particle size and smaller void diameter give the thicker capillary fringe thicknesses. The relative permeability at point (30, 50), calculated using the van Genuchten parameters, is about 0.88 (Fig. 7), confirming that the hydraulic conductivity of the unsaturated zone is close to that of the saturated zone. Lehmann et al. (1998) found that the capillary fringe thicknesses would be between 13 and 25 cm for a packed sand, and the value obtained in this experiment is within this range. As such, the process of unsaturated flow in this experiment is plausible.

Knowledge about groundwater flow paths and associations with travel time are essential to developing adequate groundwater management and protection schemes (Bekele et al. 2014; Zoellmann et al. 2001). In addition, this information is prerequisite to efficient monitoring and risk assessment. Chemical loading rates were strongly controlled by the groundwater flow paths and geochemical conditions in the aquifer (Robinson et al. 2014), particularly in the arid and semi-arid areas. Hydro-geochemical characteristics and geochemical processes within specific aquifers will be changed severely due to variations of groundwater flow paths. Just as at many sites of the world, hydro-geochemical processes have been changed by reductions in groundwater level due to human activities (Xing et al. 2013; Zhan et al. 2014; Liu et al. 2016). In addition, understanding the flow paths of ambient groundwater is essential to obtaining knowledge of the infiltrated–ambient groundwater interface areas, in which mixing of the infiltrated water and ambient groundwater always occurred and vertical stratification of the flow system exists (Moeck et al. 2017). More attention should be paid to variations in the hydro-geochemical processes at the interfaces

between infiltrated water and ambient groundwater. Furthermore, variations in soil salinity in the downstream infiltration basin or injection well should have also been considered because the soil moisture will be increased due to infiltration and water injected through the wells. Additionally, strong evaporation at the area may cause the accumulation of salts in the soil with increased soil moisture.

Notably, the groundwater flow lines could go across the water table, which is common in some conditions—for example, Newcomer et al. (2016) showed that losing rivers are particularly common in dry regions, where disconnection between the surface water and groundwater (leading to the development of an unsaturated zone) can occur. Similar to Newcomer's work, Wang et al. (2011) performed experiments on the evolution the hydrologic connectedness of the stream-aquifer during pumping. In these conditions, surface water flows through the unsaturated zone and moves across the water table to recharge the groundwater. This phenomenon is also shown in the tracer test results in the right panel in Fig. 6.

The transit or residence time of groundwater from recharge to discharge areas (Abrams 2012; Cardenas 2007; Wörman et al. 2007) determines the type and rate of many processes occurring at the surface, near the surface, and in deep environments, and involves biological (Lin et al. 2006) biogeochemical (Cardenas 2008; Hogan et al. 2007; Kirchner et al. 2000), and purely physical processes (Abrams et al. 2009; Maxwell and Kollet 2008). Short residence times might indicate that groundwater is vulnerable due to a limited amount of time for self-purification (Kralik et al. 2014); however, long residence times indicate reduced groundwater renewability (Huang et al. 2017). Spatial and temporal variations in the mean residence time are dependent on human activities such as groundwater abstraction (Toews et al. 2016). Regarding the results of this study, under the driver of artificial recharge, the flow velocities of ambient groundwater are significantly decreased, indicating a long residence time after the occurrence of artificial recharge. This result may suggest that a small ratio of ambient groundwater should be abstracted.

Groundwater age and groundwater residence time are completely different concepts. By adopting the age mass proposed by Goode (1996), groundwater age was determined with the consideration of advection, dispersion, and mixing functions; however, groundwater residence time, also called travel time and transit time, is a description of residence times of groundwater from recharge to discharge (Abrams 2012; Cardenas 2007; Wörman et al. 2007). Under the influence of the same factors, groundwater age and groundwater residence time could show different behaviors. Just as the results in this scale, groundwater age was decreased by artificial recharge, with the dispersion and mixing of infiltrated younger water. At the same time, the residence time of ambient groundwater was increased by artificial recharge especially in the upstream areas of artificial recharge projects. The existence of saddle points in flow nets is relevant to a range of geologic processes (Jiang et al. 2011). Groundwater plays an active role in certain geologic processes and has been recognized in numerous sub-disciplines (Tóth 1999). A wide range of natural processes and phenomena have thus shown flowing groundwater to be a general geologic agent. In stagnant zones, which are associated with saddle points, different groundwater flow systems converging from and parting toward opposite directions coexist. There is an accumulation of transported mineral matter such as metallic ions (uranium, sulfides), hydrocarbons, and anthropogenic contaminants, primarily in regions of converging flow paths (hydraulic traps) or in regions where the fluid potential is minimum with respect to a transported immiscible fluid (Tóth 1999). The positions of these saddle points were found to be sensitive to the water table, the hydraulic conductivity of the aquifer, the ratio of the horizontal to vertical hydraulic conductivity of the groundwater system (Winter 1976), and the depth-decay exponent of hydraulic conductivity (Jiang et al. 2011). Under artificial regulation, saddle points may exist in different locations, both in the saturated zone and unsaturated zone. These findings have implications, for example, in interpreting residence time distributions or studying potential sites of concentrating contaminants, which may exist in stagnant zones.

Conclusions

Groundwater reservoirs, which are highly dependent on artificial regulation, represent an important means of meeting water demand in regions where water resources have significant uneven distribution across time. Knowledge about the variations in ambient groundwater flow paths driven by artificial regulation and the combining effects are essential to developing practical strategies for groundwater resources planning and management. Here, a 2D laboratory sand tank and corresponding numerical simulation model based on hydrogeological conditions of the groundwater reservoir in the Tailan River Basin were developed to explore artificial regulation drivers of

groundwater flows in an inland groundwater reservoir. The laboratory experiments and numerical simulations have demonstrated that ambient groundwater flow paths were significantly changed by the effects of artificial regulation.

The presence of the abstraction led to a reduction in the soil moisture content along the studied 2D phreatic aquifer. This effect in the central area of the cone of depression was intensified when abstraction occurred at a shallow layer; however, artificial recharge via the infiltration basin or injection well was found to increase the soil moisture content in the groundwater reservoir.

This study further investigated the flow dynamic under the stress of artificial regulation, whereby the results showed the existence of stagnant zones produced by artificial regulation. With the deepening of the pumping well screen, the saddle point in the saturated zone gradually disappeared. Under the stress of artificial recharge, saddle points can also appear at different locations in the upstream direction of artificial recharge projects, both in the saturated zone and unsaturated zone. Locations of saddle points were highly dependent on the forms of artificial regulation. Thus, appropriate artificial regulation should be conducted in stagnant zones, where recharged water and ambient groundwater converging from and parting toward opposite directions coexist—for example, abstraction well fields could be drilled in the upstream of an artificial recharge area to prevent the formation of stagnant zones, which can also reduce the residence time due to artificial recharge in the upstream areas. At the exploited horizon, the abstraction needs to be adapted to the changed groundwater flow field—for example, deep-layer groundwater abstraction should be diminished with a deeper ambient groundwater penetration depth and slower velocities driven by injection at shallow layers.

It was also concluded that the artificial regulation activities have greatly changed the ambient groundwater-age and residence-time distributions in the groundwater reservoir area. This showed that groundwater abstraction and artificial recharge led to decreases in the groundwater ages in the saturated zone. Groundwater ages in the unsaturated zone near the downstream boundary were increased by abstraction but decreased by artificial recharge. The results show that not only the ambient groundwater driven by artificial regulation but also the artificial recharged water exhibit different RTD laws with the natural state. Ambient groundwater RTDs were driven by artificial recharge, and artificially recharged water RTDs show primarily exponential law behavior and logarithmic law. The deep pumping led to the FD of ambient groundwater's RTDs tending toward a logarithmic law behavior, and shallow pumping led to a polynomial motion.

The effect of abstraction on ambient groundwater flow paths primarily occurred in the cone of depression. Abstraction at the shallow layer reduced the penetration depth of the deep water and deepened the penetration depth of the shallow water in the cone of depression. With the deepening of the abstraction

depth, the penetration depth of the ambient groundwater from deep layers increased in the cone of depression. In addition, the effect of the law of artificial recharge on ambient groundwater flow paths relies on the recharge method and injection depth. The penetration depth of the ambient groundwater flow increases with the infiltration basin effect. When the injection well screen is located in the shallow layer, the penetration depth of the ambient groundwater flow increases. With the deepening of the injection well screen, the ambient groundwater flow is gradually fractionated by artificial recharge. When the injection well screen is located in the bottom layer, the penetration depth of the ambient groundwater flow decreases. To prevent the possible water quality problem produced by an interaction between the changed groundwater flow and its natural environment, alternating injections could be conducted at different depths to reduce the impact of the changed flow paths on the hydro-chemical environment.

Furthermore, water behavior in the unsaturated zone should be considered when artificially regulating in arid groundwater reservoir areas. Based on the results from laboratory experiments and numerical simulations, some artificially recharged water, especially infiltrated through the infiltration basin, is lost in the unsaturated zone, which will decrease the injection efficiency.

The dimensionality and scale of the model adopted in the current study may lead to some limitations with respect to the study result—for example, the ratio of the capillary zone thickness (17 cm) to the saturated zone thickness (50 cm) is extremely high, which would be unreasonable when considering a field-scale model of the study aquifer (i.e., the Tailan basin aquifer). However, the results obtained could offer important implications for understanding ambient groundwater flow dynamics impacted by pumping and recharge activities.

Acknowledgements The authors acknowledge the valuable comments from the reviewers, which led to significant improvement of the paper. All the authors participated in every step of this research. In particular, Peipeng Wu and Longcang Shu designed the study scheme and different scenarios and analyzed the experimental and numerical results. Peipeng Wu established the physical and numerical models and conducted the model calibration and verification. Changbing Yang co-designed and analyzed the physical model. Yang Xu designed and analyzed the regulation plan of the groundwater reservoir. Yongjie Zhang co-designed and analyzed the physical model and numerical simulation results

Funding information This research was supported by the National Natural Science Foundation of China (41572210), providing financial support for the collection of data, the writing and publishing of the results.

Compliance with ethical standards

Conflict of interest The authors declare no conflict of interest. We declare that there are no personal circumstances or interests that may be perceived as inappropriately influencing the representation or interpretation of the reported research results.

References

- Abrams D (2012) Correcting transit time distributions in coarse MODFLOW-MODPATH models. *Groundwater* 51(3):474–478. <https://doi.org/10.1111/j.1745-6584.2012.00985.x>
- Abrams DM, Lobkovsky AE, Petroff AP (2009) Growth laws for channel networks incised by groundwater flow. *Nat Geosci* 2(3):193–196
- Alley WM, Healy RW, LaBaugh JW, Thomas ER (2002) Flow and storage in groundwater systems. *Science* 296:1985–1990
- American Water Works Association (2014) M21 groundwater. AWWA, Denver, CO
- Andrew FBT, Steven FC, Nina DR, Maxwell RM (1999) Analysis of groundwater migration from artificial recharge in a large urban aquifer: a simulation perspective. *Water Resour Res* 35(10):2981–2998
- Atlabachew A, Shu L, Wu P (2018) Numerical modeling of solute transport in a sand tank physical model under varying hydraulic gradient and hydrological stresses. *Hydrogeol J* 1:1–25
- Bao ZX, Zhang JY, Wang GQ (2012) Attribution for decreasing stream flow of the Haihe River basin, northern China: climate variability or human activities. *J Hydrol* 460–461:117–129
- Barker JLB, Hassan MM, Sultana S (2016) Numerical evaluation of community-scale aquifer storage, transfer and recovery technology: a case study from coastal Bangladesh. *J Hydrol* 540:861–872
- Barnett TP, Pierce DW, Hidalgo HG (2008) Human-induced changes in the hydrology of the western United States. *Science* 319(5866):1080–1083
- Bear J (1979) *Hydraulics of groundwater*. McGraw-Hill, New York
- Bekele E, Bradley P, Simon T (2014) Aquifer residence times for recycled water estimated using chemical tracers and the propagation of temperature signals at a managed aquifer recharge site in Australia. *Hydrogeol J* 22(6):1383–1401
- Blair TC, McPherson JG (2009) Processes and forms of alluvial fans, chap 14. In: Parsons AJ, Abrahams AD (eds) *Geomorphology of desert environments*. Springer, Heidelberg, Germany, pp 413–467
- Carabin G, Dassargues A (1999) Modeling ground water with ocean and river interaction. *Water Resour Res* 35(8):2347–2358
- Cardenas MB (2007) Potential contribution of topography-driven regional groundwater flow to fractal stream chemistry: residence time distribution analysis of Tóth flow. *Geophys Res Lett* 34(5):L05403. <https://doi.org/10.1029/2006GL029126>
- Cardenas MB (2008) Surface water-groundwater interface geomorphology leads to scaling of residence times. *Geophys Res Lett* 35:L08402. <https://doi.org/10.1029/2008GL033753>
- Deng MJ (2012) Ground reservoir: a new pattern of groundwater utilization in arid North-West China: a case study in Tailan River Basin. *Procedia Environ Sci* 13:2210–2221
- Deng HJ, Chen YN (2017) Influences of recent climate change and human activities on water storage variations in Central Asia. *J Hydrol* 544:46–57
- Diersch H (2014) *FEFLOW finite element modeling of flow, mass and heat transport in porous and fractured media*. Springer, Berlin
- Dillon P (2005) Future management of aquifer recharge. *Hydrogeol J* 13:313–316
- Dillon P, Pavelic P, Toze S (2006) Role of aquifer storage in water reuse. *Desalination* 188:123–134
- Ebrahim GY, Jonoski A, Al-Maktoumi A (2016) Simulation-optimization approach for evaluating the feasibility of managed aquifer recharge in the Samail Lower Catchment, Oman. *J Water Resour Plan Manag* 142(2). [https://doi.org/10.1061/\(ASCE\)WR.1943-5452.0000588](https://doi.org/10.1061/(ASCE)WR.1943-5452.0000588)
- Emily CE, Thomas H, Graham EF (2016) Assessing the effectiveness of drywells as tools for stormwater management and aquifer recharge and their groundwater contamination potential. *J Hydrol* 539:539–553
- Erickson TO, Stefan HG (2009) Natural groundwater recharge response to urbanization: Vermillion River watershed, Minnesota. *J Water Resour Plan Manag* 135(6):512–520

- Fan L, Li H, Miguezmacho G (2013) Global patterns of groundwater table depth. *Science* 339(6122):940–943
- Frederick B, Chi HS, Joseph JD (2014) Lessons learned from aquifer storage and recovery (ASR) systems in the United States. *J Water Resour Protect* 6:1603–1629
- Gao SD, Pan L, Pan ZK (2017) Derivation of low flow frequency distributions under human activities and its implications. *J Hydrol* 549: 294–300
- Ghaleni M, Ebrahimi K (2015) Effects of human activities and climate variability on water resources in the Saveh Plain, Iran. *Environ Monit Assess* 187(2):35
- Gleeson T, Wada Y, Bierkens MF (2012) Water balance of global aquifers revealed by groundwater footprint. *Nature* 488(7410):197–200
- Goode DJ (1996) Direct simulation of groundwater age. *Water Resour Res* 32(32):289–296
- Hogan JF, Phillips FM, Mills SK (2007) Geologic origins of salinization in a semi-arid river: the role of sedimentary basin brines. *Geology* 35(12):1063–1066
- Hotta N, Tanaka N, Sawano S (2010) Changes in groundwater level dynamics after low-impact forest harvesting in steep, small watersheds. *J Hydrol* 385(1):120–131
- Huang TM, Pang ZH, Li J (2017) Mapping groundwater renewability using age data in the Baiyang alluvial fan, NW China. *Hydrogeol J* 25:743–755
- Jakobczyk-Karpierz S, Sitek S, Jakobsen R (2017) Geochemical and isotopic study to determine sources and processes affecting nitrate and sulphate in groundwater influenced by intensive human activity-carbonate aquifer Gliwice (southern Poland). *Appl Geochem* 76: 168–181
- Jia YW, Ding XY, Wang H (2012) Attribution of water resources evolution in the highly water-stressed Hai River basin of China. *Water Resour Res* 48:2513–2531
- Jiang XW, Wang XS, Wan L (2011) An analytical study on stagnation points in nested flow systems in basins with depth-decaying hydraulic conductivity. *Water Resour Res* 47:W01512. <https://doi.org/10.1029/2010WR009346>
- Jonoski A, Zhou YX, Meijer S (1997) Model-aided design and optimization of artificial recharge-pumping systems. *Hydrol Sci J* 42(6): 937–953
- Keeler BL, Gourevitch JD, Polasky S (2016) The social costs of nitrogen. *Sci Adv* 2(10):e1600219. <https://doi.org/10.1126/sciadv.1600219>
- Kirchner JW, Feng XH, Neal C (2000) Fractal stream chemistry and its implications for contaminant transport in catchments. *Nature* 403(6769):524–527
- Konrad M, Peter JD, Paul P (2014) Recovery of injected freshwater from a brackish aquifer with a multiwell system. *Groundwater* 52(4):495–502
- Kralik M, Humer F, Fank J (2014) Using $^{18}\text{O}/^{2}\text{H}$, $^3\text{H}/^3\text{He}$, ^{85}Kr and CFCs to determine mean residence times and water origin in the grazer and Leibnitzer Feld groundwater bodies (Austria). *Appl Geochem* 50: 150–163
- Lehmann P, Stauffer F, Hinz C, Dury O, Flüher H (1998) Effect of hysteresis on water flow in a sand column with a fluctuating capillary fringe. *J Contam Hydrol* 33(1):81–100
- Lin LH, Wang PL, Rumble D (2006) Long-term sustainability of a high-energy, low-diversity crustal biome. *Science* 314(5798):479–482
- Liu H, Guo H, Xing L (2016) Geochemical behaviors of rare earth elements in groundwater along a flow path in the North China plain. *J Asian Earth Sci* 117:33–51
- Maliva RG, Guo W, Missimer TM (2006) Aquifer storage and recovery: recent hydrogeological advances and system performance. *Water Environ Res* 78:2428–2435
- Maxwell RM, Kollet SJ (2008) Interdependence of groundwater dynamics and land-energy feedbacks under climate change. *Nat Geosci* 1(10):665–669
- Mi L, Xiao HL, Zhang JM (2016) Evolution of the groundwater system under the impacts of human activities in middle reaches of Heihe River basin (Northwest China) from 1985 to 2013. *Hydrogeol J* 24: 971–986
- Moeck C, Radny D, Popp A (2017) Characterization of a managed aquifer recharge system using multiple tracers. *Sci Total Environ* 609: 701–714
- Nakaya S, Uesugi K, Yusuke M (2007) Spatial separation of groundwater flow paths from a multi-flow system by a simple mixing model using stable isotopes of oxygen and hydrogen as natural tracers. *Water Resour Res* 43(9):252–258
- Newcomer ME, Hubbard SS, Fleckenstein JH (2016) Simulating bioclogging effects on dynamic riverbed permeability and infiltration. *Water Resour Res* 52:2883–2900
- Oki T, Kanae S (2006) Global hydrological cycles and world water resources. *Science* 313(5790):1068–1072
- Oostrom M, Hayworth JS, Dane JH (1992) Behavior of dense aqueous phase leachate plumes in homogeneous porous media. *Water Resour Res* 28(8):2123–2134. <https://doi.org/10.1029/92WR00711>
- Polizzotto ML, Kocar BD, Benner SG (2008) Near-surface wetland sediments as a source of arsenic release to ground water in Asia. *Nature* 454(7203):505–508
- Qin DJ, Zhao ZF, Han LF (2012) Determination of groundwater recharge regime and flow path in the lower Heihe River basin in an arid area of Northwest China by using environmental tracers: implications for vegetation degradation in the Ejina oasis. *Appl Geochem* 27:1133–1145
- Robinson C, Xin P, Li L (2014) Groundwater flow and salt transport in a subterranean estuary driven by intensified wave conditions. *Water Resour Res* 50:165–181
- Rodell M, Velicogna I, Famiglietti JS (2009) Satellite-based estimates of groundwater depletion in India. *Nature* 460:999–1002
- Sawyer AH, David CH, Famiglietti JS (2016) Continental patterns of submarine groundwater discharge reveal coastal vulnerabilities. *Science* 353(6300):705
- Stoeckl L, Houben G (2012) Flow dynamics and age stratification of freshwater lenses: experiments and modeling. *J Hydrol* 458–459: 9–15
- Toews MW, Daughney CJ, Comaton FJ (2016) Numerical simulation of transient groundwater age distributions assisting land and water management in the middle Wairarapa Valley, New Zealand. *Water Resour Res* 52:9430–9451. <https://doi.org/10.1002/2016WR019422>
- Tóth J (1999) Groundwater as a geologic agent: an overview of the causes, processes, and manifestations. *Hydrogeol J* 7(1):1–14. <https://doi.org/10.1007/s100400050176>
- Vacher HL, Hutchings WC, Budd DA (2006) Metaphors and models: the ASR bubble in the Floridan aquifer. *Ground Water* 44:144–154
- Van Genuchten MT (1980) A closed-form equation for predicting the hydraulic conductivity of unsaturated soils. *Soil Sci Soc Am J* 44(5):892–898
- Wada Y, Beek L, Kempen C (2010) Global depletion of groundwater resources. *Geophys Res Lett* 37(20):114–122
- Wada Y, Beek L, Bierkens M (2012) Nonsustainable groundwater sustaining irrigation: a global assessment. *Water Resour Res* 48(6): 335–344
- Wang GS, Xia J, Chen J (2009) Quantification of effects of climate variations and human activities on runoff by a monthly water balance model: a case study of the Chaobai River basin in northern China. *Water Resour Res* 45(7):206–216
- Wang W, Li J, Feng X (2011) Evolution of stream-aquifer hydrologic connectedness during pumping-experiment. *J Hydrol* 402:401–414
- Wang W, Li J, Wang W (2014) Estimating streambed parameters for a disconnected river. *Hydrol Process* 28:3627–3641

- Ward JD, Simmons CT, Dillon PJ (2009) Integrated assessment of lateral flow, density effects and dispersion in aquifer storage and recovery. *J Hydrol* 370:83–99
- Wilson AM, Huettel M, Klein S (2008) Grain size and depositional environment as predictors of permeability in coastal marine sands. *Estuar Coast Shelf Sci* 80(1):193–199
- Winter TC (1976) Numerical simulation analysis of the interaction of lakes and ground water. *US Geol Surv Prof Pap* 1001:1–45
- Wörman A, Marklund L, Xu S, Dverstorp B (2007) Impact of repository depth on residence times for leaking radionuclides in land-based surface water. *Acta Geophys* 55(1):73–84. <https://doi.org/10.2478/s11600-006-0040-9>
- Xing LN, Guo HM, Zhan YH (2013) Groundwater hydrochemical characteristics and processes along flow paths in the North China plain. *J Asian Earth Sci* 70–71:250–264
- Yang T, Zhang Q, Wang W (2013) Review of advances in hydrologic science in China in the last decades: impact study of climate change and human activities. *J Hydrol Eng* 18(11):1380–1384
- Zhan YH, Guo HM, Wu Y (2014) Evolution of groundwater major components in the Hebei plain: evidences from 30-year monitoring data. *J Earth Sci* 25(3):563–574
- Zhang X, Zwiers FW, Hegerl GC (2007) Detection of human influence on twentieth-century precipitation trends. *Nature* 448(7152):461–465
- Zijl W, (1999) Scale aspects of groundwater flow and transport systems. *Hydrogeology Journal* 7 (1):139-150
- Zoellmann K, Kinzelbach W, Fulda C (2001) Environmental tracer transport (H-3 and SF6) in the saturated and unsaturated zones and its use in nitrate pollution management. *J Hydrol* 240(3–4):187–205